TEKTONIKA

Total Shortening Estimates Across the Western Greater Caucasus Mountains from Balanced Cross Sections and Area Balancing

Charles C. Trexler *[1,2], **Eric S. Cowgill**[2], **Dylan A. Vasey**[2,3], **Nathan A. Niemi**[4]

[1]Earthquake Science Center, U.S. Geological Survey, Moffett Field, CA USA 94035 | [2]Department of Earth and Planetary Sciences, University of California, Davis, CA USA 95616 | [3]Department of Earth and Climate Sciences, 004 Lane Hall, Tufts University, Medford, MA USA 02155 | [4]Department of Earth and Environmental Sciences, University of Michigan, Ann Arbor, MI USA 48109

Executive Editor:
Janine Kavanagh
Associate Editor:
Chiara Montomoli
Technical Editor:
Mohamed Gouiza

Reviewers:
Anonymous 1
Anonymous 2

Submitted:
23 May 2022
Accepted:
23 November 2023
Published:
20 December 2023

Abstract The Greater Caucasus orogen forms the northern edge of the Arabia-Eurasia collision zone. Although the orogen has long been assumed to exhibit dominantly thick-skinned style deformation via reactivation of high-angle extensional faults, recent work suggests the range may have accommodated several hundred kilometers or more of shortening since its ~30 Ma initiation, and this shortening may be accommodated via thin-skinned, imbricate fan-style deformation associated with underthrusting and/or subduction. However, robust shortening estimates based upon surface geologic observations are lacking. Here we present line-length and area balanced cross sections along two transects across the western Greater Caucasus that provide minimum shortening estimates of 130-200 km. These cross sections demonstrate that a thin-skinned structural style provides a viable explanation for the structure of the Greater Caucasus, and highlight major structures that may accommodate additional, but unconstrained, shortening.

Plain Language Summary The Greater Caucasus Mountains are a young mountain range between the colliding Arabian and Eurasian tectonic plates. Arabia and Eurasia are moving toward each other and the Greater Caucasus are still growing, but where and how this convergent motion is accommodated is still a topic of debate. Recent work suggests that the mountains may be the result of several hundred to a thousand or more km of plate convergence over the past 30 million years. Here, we present models that use orientations of rock layers and faults to estimate that at least 130-200 kilometers of plate convergence has occurred during the growth of the Greater Caucasus.

1 Introduction

Despite considerable variability in structural style, convergent orogens are often classified as either "thin-skinned" or "thick-skinned" (e.g., *Mouthereau et al.*, 2013). Definitions of these styles vary, but the most widely accepted usage employs the involvement of basement in deformation as a distinguishing characteristic of thick-skinned deformation, whereas thin-skinned deformation occurs isolated from the basement below (e.g., *Rodgers*, 1949). Thin- and thick-skinned models across the same orogen can produce shortening estimates that differ by as much as an order of magnitude (e.g., *Scisciani et al.*, 2014).

Classical models of fold-thrust belts as critically tapered wedges (e.g., *Davis et al.*, 1983) deform in a thin-skinned style, where the deforming material is detached from its basement along a décollement (e.g., *Chapple*, 1978). Many collisional orogens around the world have been modeled at least in part using a thin-skinned structural style, including the North American Cordillera (e.g., *Armstrong*, 1968), Bolivian Andes (e.g., *Anderson et al.*, 2017), Bhutan Himalaya (e.g., *Long et al.*, 2011), and Pyrenees (e.g., *Seguret and Daignieres*, 1986). In the thin-skinned model, steeply dipping faults and their overlying strata are interpreted as imbricate fans in which initially shallow faults are rotated to steep dips by thrust stacking beneath them (*Boyer*, 1992; *Mitra and Sussman*, 1997). By contrast, in thick-skinned fold/thrust belts, steeply dipping faults are often interpreted as inherited rift-related extensional faults that have been reactivated with a reverse sense during subsequent convergence. Examples of this thick-skinned style include the Peruvian Eastern Cordillera (e.g., *Perez et al.*, 2016), the North American

*✉ ctrexler@usgs.gov

Laramide (e.g., *Marshak et al.*, 2000) and the Papuan Fold Belt (e.g., *Mahoney et al.*, 2017).

In thin-skinned structural systems, bedding planes or other weak horizons often function as detachment surfaces that accommodate large magnitudes of displacement, with ramps between detachment horizons associated with the formation of duplexes and imbricate fans of repeated stratigraphic section, both of which accommodate large magnitudes of shortening (e.g., *Boyer and Elliott*, 1982). In contrast, thick-skinned structural systems typically lack structurally duplicated tectonostratigraphic packages and accommodate comparatively small magnitudes of shortening (e.g., *Pfiffner*, 2006). In these reactivated rift zones, creation of steep bedding orientations using solely inversion of high angle faults often requires some combination of detachment folding and pure-shear thickening, such as that seen in the Argentinian Andes (*Giambiagi et al.*, 2008) and the Italian Apennines (*Scisciani et al.*, 2014).

The Greater Caucasus Mountains (GC), located between the Black and Caspian Seas at the northern edge of the Arabia-Eurasia collision zone (Figure 1a), are a relatively young collisional orogen, and the structural style of the GC is actively debated. The GC formed as the result of closure of a Jurassic-Cretaceous back-arc basin, generally referred to as the Greater Caucasus Basin, which opened north of the Pontide-Lesser Caucasus island arc during north-directed subduction of the Neothethys Sea (e.g., *Adamia et al.*, 1977; *Gamkrelidze*, 1986; *Zonenshain and Le Pichon*, 1986; *Adamia et al.*, 2011; *Cowgill et al.*, 2016; *Vincent et al.*, 2016; *van der Boon et al.*, 2018; *van Hinsbergen et al.*, 2020). The surface geology in the GC is characterized by steeply-dipping stratigraphic panels bounded by equally steeply dipping faults (*Mosar et al.*, 2022; *Trexler et al.*, 2022; *Tye et al.*, 2022). Importantly, the western GC can be subdivided into discrete tectonostratigraphic domains that are bounded by structures, across which there is no recognized stratigraphic continuity (*Trexler et al.*, 2022).

The GC has long been interpreted to exhibit deformation on high-angle faults (e.g., *Leonov*, 1967; *Somin and Belov*, 1967; *Schevchenko*, 1968), more recently interpreted as thick-skinned style deformation resulting from reactivation of inherited, high-angle extensional structures (e.g., *Adamia et al.*, 1977; *Vincent et al.*, 2016; *Mosar et al.*, 2022). A corollary of this interpretation is that the Greater Caucasus Basin was relatively narrow, floored by continental crust, and inverted along Mesozoic basin-bounding normal faults that reactivated as reverse faults during Cenozoic convergence (e.g., *Vincent et al.*, 2016; *Mosar et al.*, 2022).

However, recent work challenges this model. Seismicity datasets reveal subduction of possible oceanic lithosphere beneath the eastern GC (e.g., *Mumladze et al.*, 2015; *Gunnels et al.*, 2021), which suggests the basin was at least wide enough for subduction to initiate. In addition, contrasts in sedimentary provenance indicate the inverted basin was too wide for there to be sedimentary exchange between its northern and southern margins, suggesting that it was potentially hundreds of km wide (Figure 1b *Cowgill et al.*, 2016; *Tye et al.*, 2021). Structural interpretations of regional paleomagnetic data indicate upwards of 200 km of plate convergence in the GC (*van der Boon et al.*, 2018), with regional plate reconstructions allowing as much as 1000 km of plate convergence across the Greater and Lesser Caucasus combined (*Bazhenov and Burtman*, 1989; *McQuarrie and van Hinsbergen*, 2013; *Meijers et al.*, 2015) (Figure 1b). Importantly, these independent datasets demonstrate that the Greater Caucasus Basin may have been several hundred km or more in width, and that the modern orogen potentially absorbed large-magnitude shortening via thin-skinned shortening of sedimentary rocks deposited within the basin. In this alternative end-member model, the high-angle faults and steeply dipping bedding in the core of the range are not the result of normal fault reactivation and pure-shear thickening but instead represent an imbricate fan (e.g., *Trexler et al.*, 2022; *Tye et al.*, 2022) where high-angle structures result from rotation of formerly low-angle structures (e.g., *Hoth et al.*, 2007).

Although these recent datasets together demonstrate that large magnitudes of shortening are permissible within the GC, whether these estimates of significant shortening are consistent with geologic datasets from within the orogen remains an open question. Here, we leverage newly published structural datasets from the western GC (*Mosar et al.*, 2022; *Trexler et al.*, 2022) to construct line- and area-balanced cross sections across the orogen, which provide quantitative constraints on total shortening recorded in the surface geology and allow us to assess the degree to which observed shortening is consistent with these competing models for orogen evolution.

2 Geologic Background

Exhumation and uplift of the modern GC likely began at 30 Ma, based on low-temperature thermochronology studies (*Avdeev and Niemi*, 2011; *Vincent et al.*, 2011; *Vasey et al.*, 2020; *Vincent et al.*, 2020; *Tye et al.*, 2022). This timing is consistent with estimates of Arabia-Eurasia collision initiation (e.g., *McQuarrie and van Hinsbergen*, 2013) and supported by stratigraphic data from the western GC (*Vincent et al.*, 2007). The GC have likely served as the main locus of Arabia-Eurasia shortening since 10-5 Ma, as evidenced by an increase in exhumation rates at this time (e.g., *Avdeev and Niemi*, 2011; *Vasey et al.*, 2020; *Vincent et al.*, 2020; *Forte et al.*, 2022) and consistent with timing of regional plate reorganization (e.g., *Allen et al.*, 2004).

Modern tectonic activity has been documented

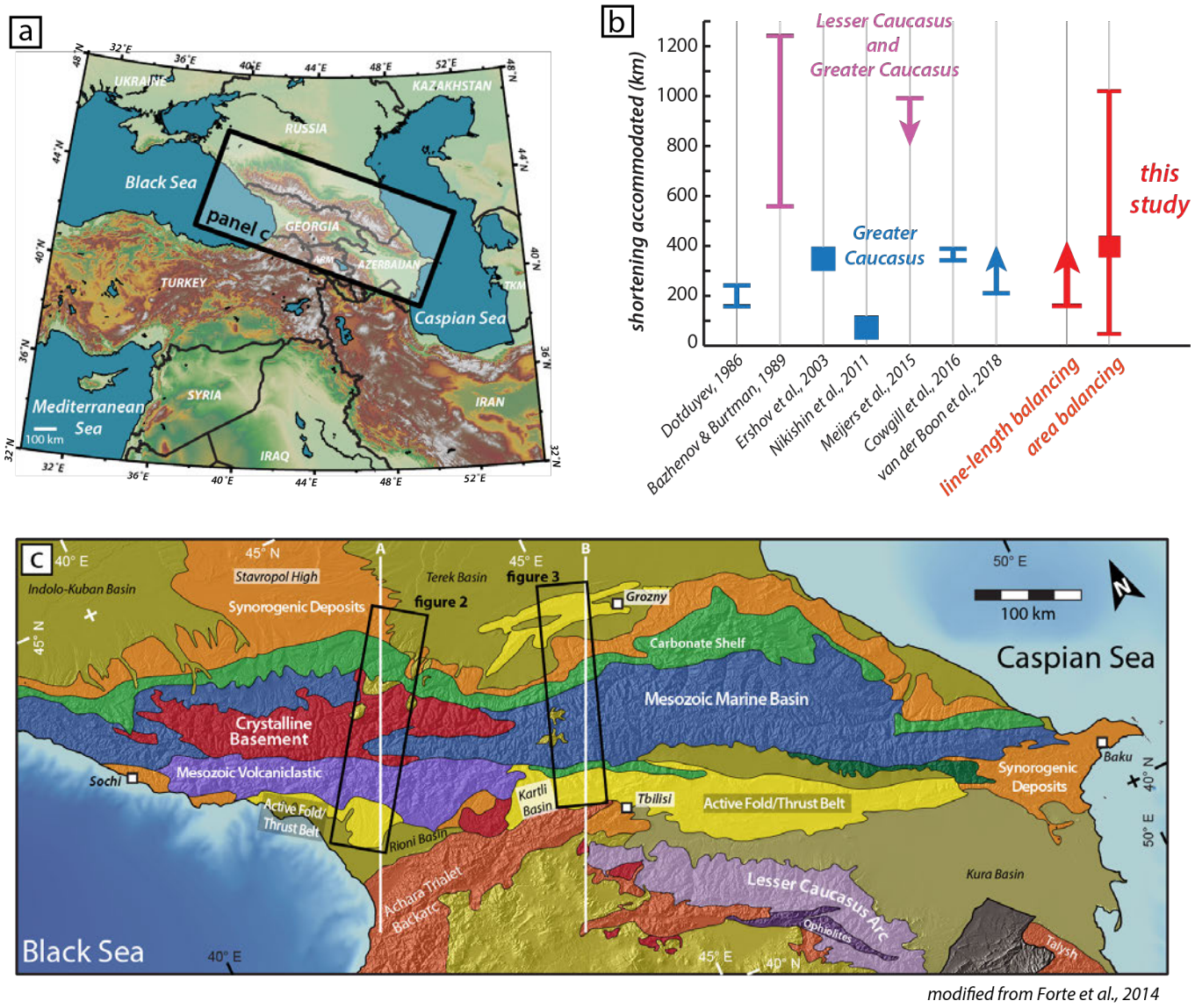

modified from Forte et al., 2014

Figure 1 – **a)** Regional map highlighting the location of the Greater Caucasus within the Arabia-Eurasia collision zone, modified from *Forte et al.* (2014). ARM – Armenia; TKM – Turkmenistan. **b)** Published estimates of shortening accommodated by the Greater Caucasus orogen, based on published structural data (*Mosar et al.*, 2022; *Trexler et al.*, 2022). **c)** Simplified tectonic map of the Greater Caucasus and surrounding region. Black rectangles show locations of cross section profiles (Figure 2 and 3); white lines show locations of area balancing profiles (Figure 4).

in the foreland fold/thrust belt on the southern flank of the range (*Forte et al.*, 2014; *Tibaldi et al.*, 2017; *Trexler et al.*, 2020; *Stahl et al.*, 2022; *Sukhishvili et al.*, 2021) but does not appear to account for all active shortening within the orogen (*Trexler et al.*, 2020; *Vasey et al.*, 2020). Along much of its length, the foreland fold-thrust belt deforms Neogene and Paleogene synorogenic deposits at the surface, though anticlines in the Rioni fold-thrust belt in western Georgia exhume strata as old as Cretaceous (*Banks et al.*, 1997; *Tibaldi et al.*, 2017).

Recent work has greatly advanced understanding of the locations and geometries of major structures within the range (*Mosar et al.*, 2022; *Trexler et al.*, 2022; *Tye et al.*, 2022) while also highlighting discrepancies in interpretations of structural style and tectonic history of the orogen. Two recent structural and tectonostratigraphic studies from the western GC report data along two roughly orogen-perpendicular transects that cross the southern half of the orogen, following the Enguri River in western Georgia (*Trexler et al.*, 2022) and the Aragvi and Terek Rivers in eastern Georgia (*Mosar et al.*, 2022; *Trexler et al.*, 2022). The interior of the range exposes primarily Mesozoic-aged marine sedimentary rocks deposited in the GC back-arc basin (*Dzhanelidze and Kandelaki*, 1957; *Kandelaki and Kakhadze*, 1957; *Gubkina and Ermakov*, 1989; *Banks et al.*, 1997; *Adamia et al.*, 2011). From south to north, both transects record a broad increase in metamorphic grade and steepening of structural orientations toward the interior of the range (*Mosar et al.*, 2022; *Trexler et al.*, 2022). Along both traverses, stratigraphic packages are subdivided by major faults, collectively referred to by *Trexler et al.* (2022) as the North Georgia Fault System (NGFS). These major faults demarcate transitions between discrete tectonostratigraphic domains distinguished

on the basis of distinct lithologic characteristics and metamorphic grade. Individually, these faults juxtapose domains that may represent spatially, as well as temporally, distinct depocenters within the larger Greater Caucasus basin during its evolution since at least the Triassic (e.g., *van Hinsbergen et al.*, 2020; *Vasey et al.*, 2021; *Darin and Umhoefer*, 2022). Along the two traverses, the faults of the NGFS are primarily inferred via abrupt changes in rock type, metamorphic grade, and internal structure. Tectonostratigraphic units are routinely truncated by NGFS structures and cannot be correlated across them (*Trexler et al.*, 2022). The northernmost fault of the NGFS, elsewhere referred to as the Main Caucasus Thrust (see *Dotduyev*, 1986; *Mosar et al.*, 2022), juxtaposes Paleozoic crystalline rock in the hanging wall against Mesozoic metasedimentary rocks in the footwall and likely accommodates some Cenozoic shortening (*Vasey et al.*, 2020).

North of the crystalline core, a north-dipping package of Mesozoic sedimentary rocks defines the northern slope of the GC and is disrupted by relatively few faults compared to the southern slope. The flanking Terek/Sunzha fold/thrust belt accommodates active shortening on the northern margin of central and eastern GC (*Sobornov*, 1994, 1996; *Forte et al.*, 2014), but does not extend west of ~44°E.

Crustal thickness in the GC ranges from 36 km in the western part of the orogen to nearly 50 km in the east, as constrained by regional tomographic studies (*Zor*, 2008). Deep (>150 km) seismicity beneath the eastern part of the range has been interpreted as evidence of subduction during basin closure, with the notable absence of deep earthquakes beneath the western half of the range inferred to be the result of recent slab detachment (*Mumladze et al.*, 2015). This model has since been reinforced by documentation of oceanic lithosphere beneath the Kura foreland basin in the eastern GC (*Gunnels et al.*, 2021), and has been suggested to explain geochemical signatures of arc magmatism found in the GC (*Vasey et al.*, 2021) and significant plate convergence between the Greater and Lesser Caucasus inferred by paleomagnetism datasets (*van der Boon et al.*, 2018) and plate boundary reconstruction studies (*Darin and Umhoefer*, 2022).

3 Shortening Estimates

Here we report independent sets of shortening estimates obtained using both line-length and area-balanced crustal-scale cross sections. Our cross sections cross the full width of the Greater Caucasus, and follow the Enguri transect of Trexler et al. (2022) and the Georgian Military Highway/Aragvi-Terek transect of Trexler et al. (2022) and Mosar et al. (2022). The stratigraphic and structural data used in construction of the balanced cross sections are previously published by Trexler et al. (2022) (figure S1, S2, and supplementary materials). Details of balanced cross section construction and restoration are provided in the supplementary materials, along with a discussion of the various assumptions made in each approach.

3.1 Line-length Balancing

When restored to pre-deformed length, the Enguri cross section records a minimum of 130 km of shortening (at least 57% of total modern orogenic width; Figure 2). The restored Aragvi-Terek cross section records a minimum of 200 km of shortening (at least 105% of total modern orogenic width; Figure 3).

With few exceptions, faults in the GC are not directly exposed and preservation of diagnostic structural features such as hanging wall or footwall cutoffs is uncommon, requiring that we make inferences about the structural style from data within fault blocks rather than directly adjacent to the faults themselves (e.g., *Trexler et al.*, 2022). Meanwhile, published subsurface data are limited to foreland basins and document that deformation is localized on bedding-subparallel detachments, even in the immediate vicinity of normal faults (*Banks et al.*, 1997). This thin-thrust-sheet-style deformation is evident in the Rioni, Kartli, and Kura basins along the southern flank of the GC, as well as in the Sunzha/Terek system on the northern flank of the GC (*Sobornov*, 1994, 1996; *Forte et al.*, 2014; *Alania et al.*, 2017; *Tibaldi et al.*, 2017; *Trexler et al.*, 2020).

Along each traverse, our cross sections highlight major structures within the North Georgia Fault System across which exposed units cannot be correlated. In most cases, these faults match previously identified major structures within the range (*Trexler et al.*, 2022; *Mosar et al.*, 2022). For the purposes of cross section restoration and shortening estimates, and to serve as a first-order permissibility test, we make approximate structural depth correlations across these structures based upon published thermochronology data (Figures 2 and 3) (*Avdeev and Niemi*, 2011; *Vincent et al.*, 2016; *Vasey et al.*, 2020; *Vincent et al.*, 2020; *Forte et al.*, 2022; *Trexler et al.*, 2022). We explicitly do not intend to imply any direct unit correlations across structures and intentionally treat each tectonostratigraphic block (bound on either side by one of these major structures) independently in restorations.

3.2 Area Balancing

We also estimate shortening using area balanced cross sections across the orogen along the same transects as our line-length balanced sections (Figure 4; Table 1). The type and thickness of the basement that floored the GC back arc basin remain disputed, and inferences range from extended continental to oceanic crust (*Mosar et al.*, 2010; *Cowgill et al.*, 2016; *Vasey et al.*, 2021). Using a range of estimated initial crustal thicknesses that

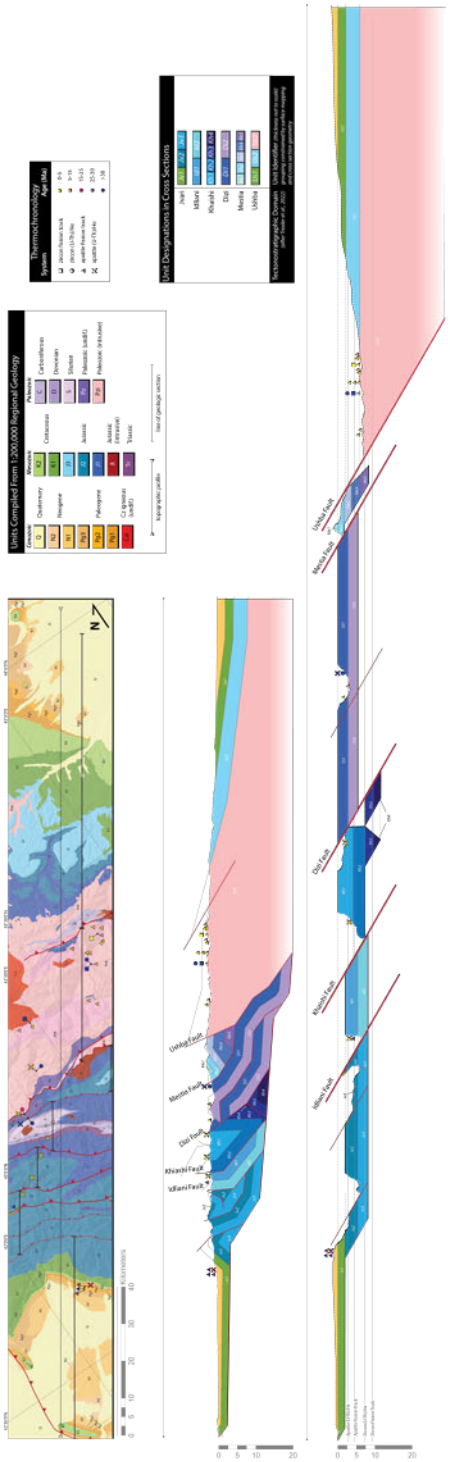

Figure 2 – Map, balanced cross section, and restored cross section for the Enguri transect, western Greater Caucasus. See Figure 1c for location. Geologic map and thermochronology data compilation by *Trexler et al.* (2022), and reproduced in Figures SI-1 and SI-2. Thermochronology symbols above cross sections are placed above the approximate sample location projected into the line of section; samples greater than 10 km from section line omitted. Grey lines in restored section (bottom) indicate approximate depth of closure window for low-temperature thermochronometers, assuming a geothermal gradient of 25°C/km and the following closure temperatures: apatite (U-Th)/He, 70°C; apatite fission track, 120□C; zircon (U-Th)/He, 200°C; zircon fission track, 210°C (*Reiners and Brandon*, 2006).

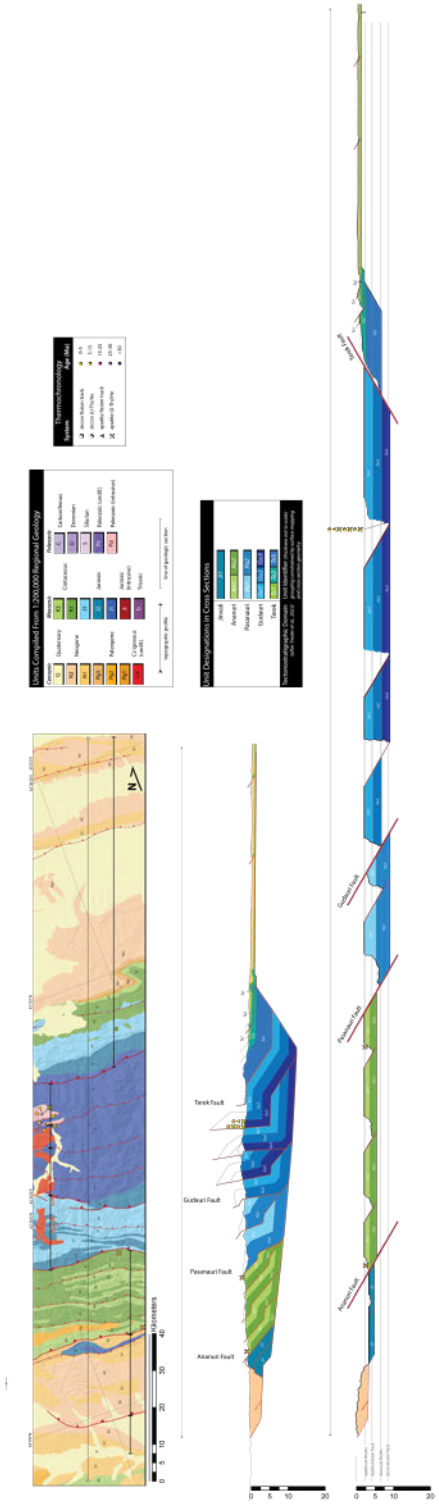

Figure 3 – Map, balanced cross section, and restored cross section for the Aragvi-Terek transect, western Greater Caucasus. See Figure 1c for location. Geologic map and thermochronology data compilation by *Trexler et al.* (2022), and reproduced in Figures SI-3 and SI-4. Thermochronology symbols above cross sections are placed above the approximate sample location projected into the line of section; samples greater than 10 km from section line omitted. Grey lines in restored section (bottom) indicate approximate depth of closure window for low-temperature thermochronometers, assuming a geothermal gradient of 25°C/km and closure temperatures reported by *Reiners and Brandon* (2006).

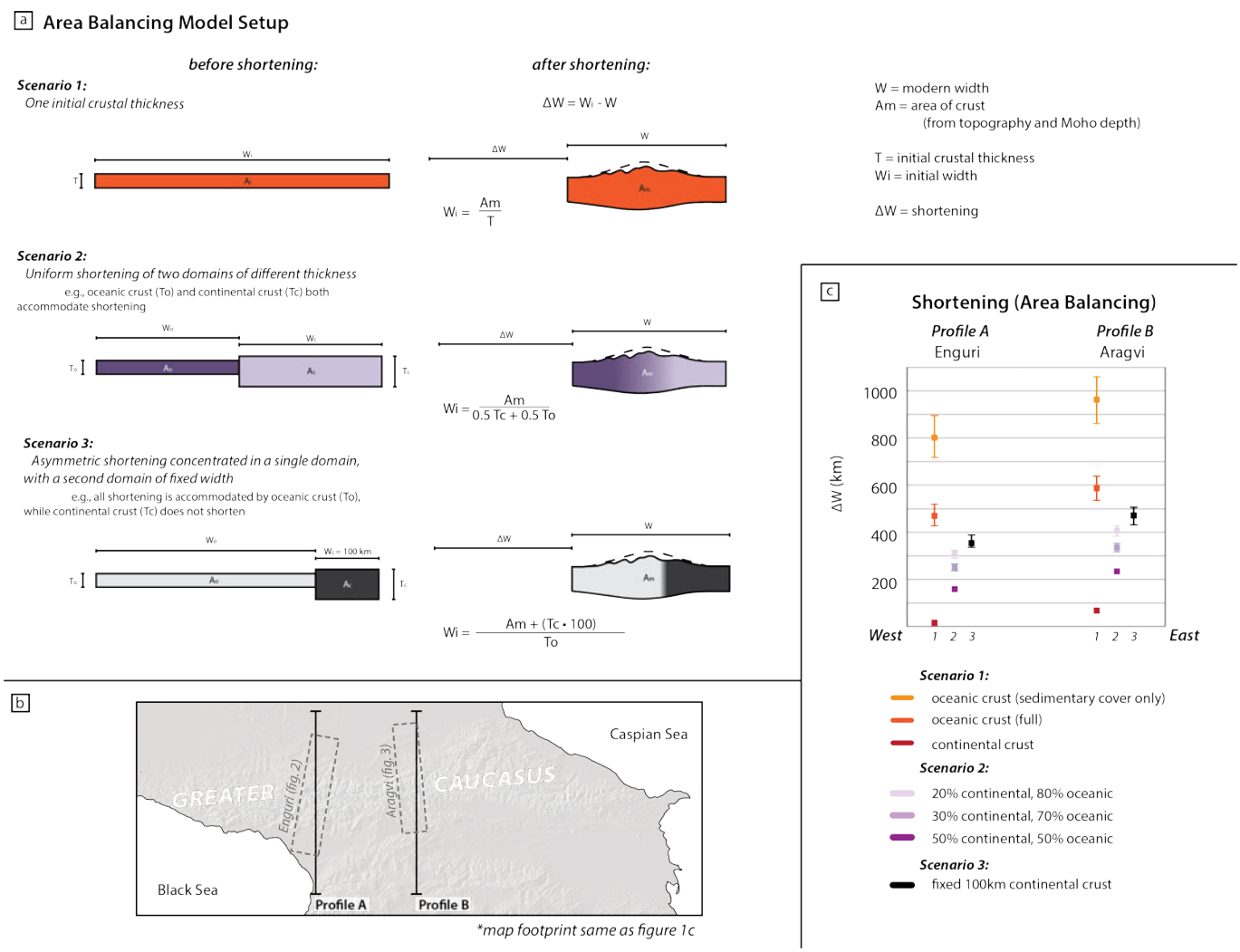

Figure 4 – **a)** Model and input parameters for area balancing. **b)** Locations of area balancing profiles. Profile A roughly aligns with the Enguri cross section (Figure 2), while Profile B roughly aligns with the Aragvi cross section (Figure 3). **c)** Results of area balancing exercise for the western Greater Caucasus orogen.

span these continental and oceanic end-members (*Yegorova and Gobarenko*, 2010) and tomographic constraints on the modern Moho geometry (*Zor*, 2008), we calculate the original length of crust required to account for the observed modern cross-sectional area, differencing the lengths of the initial and current sections to estimate shortening. To minimize shortening, we assume no loss of crust via subduction, erosion, or along-strike flux of material out of the plane of the sections.

Our area balancing models can accommodate shortening ranging from less than 100 km to nearly 1000 km, depending on the thickness of marine sedimentary units, overall crustal thickness, and the relative proportions of oceanic and continental crust along the profile (Table 1). We define a preferred area-balancing model based on geologic observations along both traverses (*Dzhanelidze and Kandelaki*, 1957; *Potapenko*, 1964; *Mosar et al.*, 2022; *Trexler et al.*, 2022), where we interpret the northernmost structure of the NGFS as the simplified boundary between the southern (oceanic crust) and northern (continental crust) domains. In our preferred model, we assign 80% of the modern orogen to material from the southern (oceanic) plate, while material from the northern (continental) plate makes up the remaining 20%. This model predicts ~400 km of shortening in the western and central GC (Figure 4). We note that this model does not include additional unrecorded shortening in the form of material lost via erosion or subduction. Thus, the shortening estimates based on our cross sections are not required to match estimates of total plate convergence from paleomagnetism (e.g., *van der Boon et al.*, 2018) or plate circuit reconstructions (e.g., *McQuarrie and van Hinsbergen*, 2013; *Meijers et al.*, 2015), which would include erosion or subduction across the convergent system.

4 Implications for Orogen Evolution

Our shortening estimates serve as a minimum bound on width of the GC back-arc basin and are of the same order of magnitude as recent estimates from paleomagnetism and plate circuit studies suggesting anywhere from ~200–1000 km of shortening across the orogen (Figure 1 *McQuarrie and van Hinsbergen*,

Table 1 – Input and output values for area balancing across the Greater Caucasus

		Profile A	Profile B
input			
W		400	400
To (full crust)*		17-19 km	17-19 km
To (sedimentary cover)*		12-14 km	12-14 km
Tc**		~39 km	~39 km
Am***		15243	17293
calculated			
Δ - scenario 1	oceanic crust (full) [km]	474	589
	oceanic crust (sedimentary cover) [km]	805	963
	continental crust [km]	16	68
Δ - scenario 2	50% continental crust, 50% oceanic crust [km]	160	232
	30% continental crust, 70% oceanic crust [km]	253	337
	20% continental crust, 80% oceanic crust [km]	313	405
Δ - scenario 3	100 km continental crust (fixed) [km]	357	471

* Oceanic sedimentary and crustal thicknesses estimated based on values from the Eastern Black Sea Basin (*Yegorova and Gobarenko*, 2010).
** Continental crustal thickness estimated based on the approximated thickness of the Scythian Platform to the north of the Greater Caucasus (*Yegorova and Gobarenko*, 2010).
*** Areas calculated using topographic profiles from ASTER digital elevation models and Moho depths from *Zor* (2008).

2013; *Meijers et al.*, 2015; *van der Boon et al.*, 2018). Our estimates are at the low end of reported ranges from those studies, consistent with our intention that our estimates provide minimum shortening values across the GC. Importantly, our cross sections allow for additional shortening via underthrusting or subduction along one or several of the faults within the NGFS, providing a mechanism wherein these models could easily accommodate several hundred km or more of additional shortening, consistent with prior work that has suggested 350 km of total shortening across the GC (*Cowgill et al.*, 2016; *van der Boon et al.*, 2018; *Darin and Umhoefer*, 2022). A significant magnitude of shortening via underthrusting or subduction may even be expected, particularly along the central GC transect, where a north-dipping zone of seismicity in the mantle delineates a subducting plate (e.g., *Mumladze et al.*, 2015).

The cross sections presented here build upon the NGFS framework of *Trexler et al.* (2022) and provide a model for the underlying architecture of the GC orogenic system. Our cross sections do not present clear support for either in- or out-of-sequence thrust sheet emplacement, consistent with low-temperature thermochronology studies that suggest simultaneous Cenozoic activity on more than one structure in the GC (e.g., *Vasey et al.*, 2020). In the structural model presented here, the western GC functions structurally as a south-vergent imbricate fan, with larger magnitudes of exhumation and steeper bedding dips in the core of the range than on the southern flank. This view of orogenic architecture is consistent with recently published structural datasets (*Mosar et al.*, 2022; *Trexler et al.*, 2022) and with low temperature thermochronologic data from the orogen, which record deeper exhumation in the core of the range than along its southern flank (e.g., *Corrado et al.*, 2021; *Vincent et al.*, 2020; *Trexler et al.*, 2022).

In addition, we suggest that our shortening estimates can be combined with temporal constraints on orogen development to provide further insights into the evolution of the modern GC. For example, our shortening estimates can be combined with published low-temperature thermochronology constraints on exhumation timing (e.g., *Avdeev and Niemi*, 2011; *Vasey et al.*, 2020; *Vincent et al.*, 2020; *Forte et al.*, 2022) to provide a first-order bound on the long-term shortening rate across the orogen. Integrated since an initiation age of ~30 Ma, the minimum shortening of 130-200 km we report implies a minimum average shortening rate of at least 4.3 mm/yr along the Enguri transect and at least 6.7 mm/yr along the Aragvi/Terek transect. Such minimum rates, particularly along the Aragvi/Terek transect, are at the high end or greater than those determined from geodetic data, which provide a modeled active convergence rate of 3-5 mm/yr in the western GC (*Sokhadze et al.*, 2018).

A decrease in cross-orogen shortening rate from the 30 Ma average to the modern geodetic rate is consistent with, while not uniquely diagnostic of, the process of subduction termination and continental collision proposed for the GC orogen (*Mumladze et al.*, 2015), and this model of tectonic evolution would additionally provide a mechanism

for juxtaposing different exhumation depths across structures, a phenomenon seen in both cross sections. Additional shortening accommodated by subduction would also provide a mechanism for bridging the gap between crustal shortening and total plate convergence estimates across the Caucasus system (e.g., Figure 1b). Additional work in collision zones such as the GC may further illuminate the relationship between shortening rate, geodynamic processes, and collisional orogen evolution.

5 Conclusion

Building upon recently published structural datasets from the western GC (*Mosar et al.*, 2022; *Trexler et al.*, 2022), we report shortening estimates from balanced cross sections that record a minimum of 130-200 km of shortening. These cross sections demonstrate that a thin-skinned structural style can reasonably reproduce geologic observations in this orogen, and produce shortening magnitudes consistent with shortening values derived from regional tectonic reconstructions derived using paleomagnetic bounds on the total width of the consumed GC basin (< 1000 km; *Meijers et al.*, 2015) and the magnitude of oroclinal bending and tectonic block rotation in the Pontides to the south of the GC (> 200 km; *van der Boon et al.*, 2018). Our shortening estimates, constrained by surface geology, fill an important gap in reconstructing the evolution of the Arabia-Eurasia collision over the Cenozoic. In addition, our balanced sections highlight a subset of structures that we suggest may accommodate additional, unconstrained shortening. These major structures are largely consistent with the North Georgia Fault System of *Trexler et al.* (2022).

Acknowledgements

This work was supported by research grants to Trexler from the Geological Society of America, the American Association of Petroleum Geologists, the Evolving Earth Foundation, and the Achievement Rewards for College Scientists Foundation. This material is based upon work supported by the National Science Foundation (NSF) under grant numbers 0810285 and 1524631 to Cowgill and 0810067 and 1524304 to Niemi from the EAR-Tectonics program, with support from the Office of International Science and Engineering. We thank Giorgi Boichenko, Mamuka Natsvilishvili, Salome Gogoladze, and Alex Tye for their assistance with field work. We also thank Adam Forte for his invaluable assistance and advice in the field and throughout the preparation of this manuscript. Any use of trade, firm, or product names is for descriptive purposes only and does not imply endorsement by the U.S. Government.

Author contributions

CT designed the study under the guidance of **EC**, and constructed the models. **EC**, **NN**, and **DV** helped interpret results and refine the study. **CT** wrote the manuscript, with assistance from **DV**. **EC** and **NN** provided revisions and editorial advice.

Data availability

All stratigraphic and structural data used and presented in this study are previously published by Trexler et al. (2022) (https://doi.org/10.1130/GES02385.1). Structural orientation data are available for download in the Supporting Information.

Competing interests

The authors declare that they have no competing interests.

Peer review

This publication was peer-reviewed by two anonymous reviewers. The full peer-review report can be found here: tektonika.online/index.php/home/article/view/50/61

Copyright notice

References

Adamia, S., G. Zakariadze, T. Chkhotua, N. Sadradze, N. Tsereteli, A. Chabukiani, and A. Gventsadze (2011), Geology of the Caucasus: A Review, *Turkish Journal of Earth Sciences*, *20*(5), 489–544, doi: 10.3906/yer-1005-11.

Adamia, S. A., M. B. Lordkipanidze, and G. S. Zakariadze (1977), Evolution of an active continental margin as exemplified by the Alpine history of the Caucasus, *Tectonophysics*, *40*(3), 183–199, doi: 10.1016/0040-1951(77)90065-8.

Alania, V. M., A. O. Chabukiani, R. L. Chagelishvili, O. V. Enukidze, K. O. Gogrichiani, A. N. Razmadze, and N. S. Tsereteli (2017), Growth structures, piggy-back basins and growth strata of the Georgian part of the Kura foreland fold–thrust belt: implications for Late Alpine kinematic evolution, https://www.lyellcollection.org/doi/full/10.1144/SP428.5, doi: 10.1144/SP428.5, accessed: 2023-11-28.

Allen, M., J. Jackson, and R. Walker (2004), Late cenozoic reorganization of the Arabia-Eurasia collision and the comparison of short-term and long-term deformation rates, *Tectonics*, *23*(2), doi: 10.1029/2003tc001530.

Anderson, R. B., S. P. Long, B. K. Horton, A. Z. Calle, and V. Ramirez (2017), Shortening and structural architecture of the Andean fold-thrust belt of southern Bolivia (21°S): Implications for kinematic development and crustal thickening of the central Andes, *Geosphere*, *13*(2), 538–558, doi: 10.1130/GES01433.1.

Armstrong, R. L. (1968), Sevier Orogenic Belt in Nevada and Utah, *GSA Bulletin*, *79*(4), 429–458, doi: 10.1130/0016-7606(1968)79[429:SOBINA]2.0.CO;2.

Avdeev, B., and N. A. Niemi (2011), Rapid Pliocene exhumation of the central Greater Caucasus constrained by low-temperature thermochronometry, *Tectonics*, *30*(2), doi: 10.1029/2010TC002808.

Banks, C. J., A. G. Robinson, and M. P. Williams (1997), Chapter 17: Structure and Regional Tectonics of the Achara-Trialet Fold Belt and the Adjacent Rioni and Kartli Foreland Basins, Republic of Georgia, *AAPG Memoir 68: Regional and Petroleum Geology of the Black Sea and Surrounding Region*, pp. 331–346.

Bazhenov, M. L., and V. S. Burtman (1989), Palaeomagnetism of Upper Cretaceous rocks from the Caucasus and its implications for tectonics, *Tectonic Evolution of the Tethyan Region*, pp. 217–239.

Boyer, S. E. (1992), Geometric evidence for synchronous thrusting in the southern Alberta and northwest Montana thrust belts, *Thrust tectonics*, pp. 377–390.

Boyer, S. E., and D. Elliott (1982), Thrust systems, *AAPG bulletin*, *66*, doi: 10.1306/03b5a77d-16d1-11d7-8645000102c1865d.

Chapple, W. M. (1978), Mechanics of thin-skinned fold-and-thrust belts, *Geological Society of America bulletin*, *89*(8), 1189, doi: 10.1130/0016-7606(1978)89<1189:motfb>2.0.co;2.

Corrado, S., T. Gusmeo, A. Schito, V. Alania, O. Enukidze, E. Conventi, and W. Cavazza (2021), Validating far-field deformation styles from the Adjara-Trialeti fold-and-thrust belt to the Greater Caucasus (Georgia) through multi-proxy thermal maturity datasets, *Marine and Petroleum Geology*, *130*, 105,141, doi: 10.1016/j.marpetgeo.2021.105141.

Cowgill, E., A. M. Forte, N. Niemi, B. Avdeev, A. Tye, C. Trexler, Z. Javakhishvili, M. Elashvili, and T. Godoladze (2016), Relict basin closure and crustal shortening budgets during continental collision: An example from Caucasus sediment provenance, *Tectonics*, *35*(12), 2918–2947, doi: 10.1002/2016tc004295.

Darin, M. H., and P. J. Umhoefer (2022), Diachronous initiation of Arabia–Eurasia collision from eastern Anatolia to the southeastern Zagros Mountains since middle Eocene time, *International geology review*, *64*(18), 2653–2681, doi: 10.1080/00206814.2022.2048272.

Davis, D., J. Suppe, and F. A. Dahlen (1983), Mechanics of fold-and-thrust belts and accretionary wedges, *Journal of geophysical research*, *88*(B2), 1153–1172, doi: 10.1029/jb088ib02p01153.

Dotduyev, S. I. (1986), The nappe structure of the Great Caucasus (in Russian), *Geotektonika*, *5*, 94–105.

Dzhanelidze, A., and N. Kandelaki (1957), Geological map of the USSR, Caucasus series sheet K-38-XIII, scale 1: 200,000, *Ministry of Geology and Mineral Protection*, *1369*.

Forte, A. M., E. Cowgill, and K. X. Whipple (2014), Transition from a singly vergent to doubly vergent wedge in a young orogen: The Greater Caucasus, *Tectonics*, *33*(11), 2077–2101, doi: 10.1002/2014TC003651.

Forte, A. M., K. R. Gutterman, M. C. van Soest, and K. Gallagher (2022), Building a young mountain range: Insight into the growth of the greater caucasus mountains from detrital zircon (U-Th)/He thermochronology and ^{10}be erosion rates, *Tectonics*, *41*(5), doi: 10.1029/2021tc006900.

Gamkrelidze, I. P. (1986), Geodynamic evolution of the Caucasus and adjacent areas in Alpine time, *Tectonophysics*, *127*(3-4), 261–277, doi: 10.1016/0040-1951(86)90064-8.

Giambiagi, L., F. Bechis, V. García, and A. H. Clark (2008), Temporal and spatial relationships of thick- and thin-skinned deformation: A case study from the malargüe fold-and-thrust belt, southern central andes, *Tectonophysics*, *459*(1), 123–139, doi: 10.1016/j.tecto.2007.11.069.

Gubkina, A. N., and V. A. Ermakov (1989), Geological Map of the USSR, Caucasus Series Sheet K-38-IX, Geological Map of the USSR, *USSR Ministry of Geology, Leningrad*.

Gunnels, M., G. Yetrimishli, S. Kazimova, and E. Sandvol (2021), Seismotectonic evidence for subduction beneath the Eastern Greater Caucasus, *Geophysical Journal International*, *224*(3), 1825–1834, doi: 10.1093/gji/ggaa522.

Hoth, S., A. Hoffmann-Rothe, and N. Kukowski (2007), Frontal accretion: An internal clock for bivergent wedge deformation and surface uplift, *Journal of Geophysical Research, [Solid Earth]*, *112*(B6), doi: 10.1029/2006JB004357.

Kandelaki, D. N., and I. R. Kakhadze (1957), Geological map of the USSR, Caucasus series sheet K-38-XV, scale 1: 200,000, *Ministry of Geology and Mineral Protection*, *1369*.

Leonov, Y. G. (1967), Tectonics of the lower-middle Jurassic sediments in the eastern part of the central Caucasus, *Geotectonics/Geotektonika*, *1*, 152–159.

Long, S., N. McQuarrie, T. Tobgay, and D. Grujic (2011), Geometry and crustal shortening of the Himalayan fold-thrust belt, eastern and central Bhutan, *GSA Bulletin*, *123*(7-8), 1427–1447, doi: 10.1130/B30203.1.

Mahoney, L., K. Hill, S. McLaren, and A. Hanani (2017), Complex fold and thrust belt structural styles: Examples from the Greater Juha area of the Papuan Fold and Thrust Belt, Papua New Guinea, *Journal of Structural Geology*, *100*, 98–119, doi: 10.1016/j.jsg.2017.05.010.

Marshak, S., K. Karlstrom, and J. M. Timmons (2000), Inversion of Proterozoic extensional faults: An explanation for the pattern of Laramide and Ancestral Rockies intracratonic deformation, United States, *Geology*, *28*(8), 735, doi: 10.1130/0091-7613(2000)28<735:iopefa>2.0.co;2.

McQuarrie, N., and D. J. J. van Hinsbergen (2013), Retrodeforming the Arabia-Eurasia collision zone: Age of collision versus magnitude of continental subduction, *Geology*, *41*(3), 315–318, doi: 10.1130/G33591.1.

Meijers, M. J. M., B. Smith, U. Kirscher, M. Mensink, M. Sosson, Y. Rolland, A. Grigoryan, L. Sahakyan, A. Avagyan, C. Langereis, and C. Müller (2015), A paleolatitude reconstruction of the South Armenian Block (Lesser Caucasus) for the Late Cretaceous: Constraints on the Tethyan realm, *Tectonophysics*, *644-645*, 197–219, doi: 10.1016/j.tecto.2015.01.012.

Mitra, G., and A. J. Sussman (1997), Structural evolution of connecting splay duplexes and their implications for critical taper: an example based on geometry and

kinematics of the canyon range culmination, sevier belt, central utah, *Journal of Structural Geology*, *19*(3-4), 503–521, doi: 10.1016/s0191-8141(96)00108-3.

Mosar, J., T. Kangarli, M. Bochud, U. A. Glasmacher, A. Rast, M.-F. Brunet, and M. Sosson (2010), Cenozoic-Recent tectonics and uplift in the Greater Caucasus: a perspective from Azerbaijan, https://www.lyellcollection.org/doi/10.1144/SP340.12, doi: 10.1144/SP340.12, accessed: 2023-11-28.

Mosar, J., J. Mauvilly, K. Koiava, I. Gamkrelidze, N. Enna, V. Lavrishev, and V. Kalberguenova (2022), Tectonics in the greater caucasus (georgia – russia): From an intracontinental rifted basin to a doubly verging fold-and-thrust belt, *Marine and Petroleum Geology*, *140*, 105,630, doi: 10.1016/j.marpetgeo.2022.105630.

Mouthereau, F., A. B. Watts, and E. Burov (2013), Structure of orogenic belts controlled by lithosphere age, *Nature geoscience*, *6*(9), 785–789, doi: 10.1038/ngeo1902.

Mumladze, T., A. M. Forte, E. S. Cowgill, C. C. Trexler, N. A. Niemi, M. Burak Yıkılmaz, and L. H. Kellogg (2015), Subducted, detached, and torn slabs beneath the Greater Caucasus, *GeoResJ*, *5*, 36–46, doi: 10.1016/j.grj.2014.09.004.

Perez, N. D., B. K. Horton, N. McQUARRIE, K. Stübner, and T. A. Ehlers (2016), Andean shortening, inversion and exhumation associated with thin- and thick-skinned deformation in southern Peru, *Geological magazine*, *153*(5-6), 1013–1041, doi: 10.1017/S0016756816000121.

Pfiffner, O. A. (2006), Thick-skinned and thin-skinned styles of continental contraction, in *Styles of Continental Contraction*, pp. 153–177, Geological Society of America, doi: 10.1130/2006.2414(09).

Potapenko, Y. Y. (1964), Geological map of the USSR, Caucasus Series Sheet K-38-I, 1:200,000 scale, *Caucasus series sheet K-38-I, scale*, *1*(200,000).

Reiners, P. W., and M. T. Brandon (2006), USING THERMOCHRONOLOGY TO UNDERSTAND OROGENIC EROSION, *Annual review of earth and planetary sciences*, *34*(1), 419–466, doi: 10.1146/annurev.earth.34.031405.125202.

Rodgers, J. (1949), Evolution of thought on structure of middle and southern Appalachians, *AAPG Bulletin*, *33*(10), 1643–1654.

Schevchenko, V. I. (1968), The Kazbek intersection of the central Caucasus (New data and a possible interpretation), *Geotectonics/Geotektonika*, *1*, 50–57.

Scisciani, V., S. Agostini, F. Calamita, P. Pace, A. Cilli, I. Giori, and W. Paltrinieri (2014), Positive inversion tectonics in foreland fold-and-thrust belts: A reappraisal of the Umbria–Marche Northern Apennines (Central Italy) by integrating geological and geophysical data, *Tectonophysics*, *637*, 218–237, doi: 10.1016/j.tecto.2014.10.010.

Seguret, M., and M. Daignieres (1986), Crustal scale balanced cross-sections of the Pyrenees; discussion, *Tectonophysics*, *129*(1), 303–318, doi: 10.1016/0040-1951(86)90258-1.

Sobornov, K. O. (1994), Structure and petroleum potential of the Dagestan thrust belt, northeastern Caucasus, Russia, *Bulletin of Canadian Petroleum Geology*, *42*(3), 352–364.

Sobornov, K. O. (1996), Lateral variations in structural styles of tectonic wedging in the northeastern Caucasus, Russia, *Bulletin of Canadian Petroleum Geology*, *44*(2), 385–399.

Sokhadze, G., M. Floyd, T. Godoladze, R. King, E. S. Cowgill, Z. Javakhishvili, G. Hahubia, and R. Reilinger (2018), Active convergence between the Lesser and Greater Caucasus in Georgia: Constraints on the tectonic evolution of the Lesser–Greater Caucasus continental collision, *Earth and planetary science letters*, *481*, 154–161, doi: 10.1016/j.epsl.2017.10.007.

Somin, M. L., and A. A. Belov (1967), On the tectonic history of the southern slope of the Greater Caucasus, *Geotectonics/Geotektonika*, *1*, 37–39.

Stahl, T. A., E. Cowgill, G. Boichenko, D. A. Vasey, and T. Godoladze (2022), Recent surface rupturing earthquakes along the south flank of the greater caucasus near tbilisi, georgia, *Bulletin of the Seismological Society of America*, *112*(4), 2170–2188, doi: 10.1785/0120210267.

Sukhishvili, L., A. M. Forte, G. Merebashvili, J. Leonard, K. X. Whipple, Z. Javakhishvili, A. Heimsath, and T. Godoladze (2021), Active deformation and Plio-Pleistocene fluvial reorganization of the western Kura fold–thrust belt, Georgia: implications for the evolution of the Greater Caucasus Mountains, *Geological magazine*, *158*(4), 583–597, doi: 10.1017/S0016756820000709.

Tibaldi, A., V. Alania, F. L. Bonali, O. Enukidze, N. Tsereteli, N. Kvavadze, and O. Varazanashvili (2017), Active inversion tectonics, simple shear folding and back-thrusting at Rioni Basin, Georgia, *Journal of Structural Geology*, *96*, 35–53, doi: 10.1016/j.jsg.2017.01.005.

Trexler, C. C., E. Cowgill, J. Q. G. Spencer, and T. Godoladze (2020), Rate of active shortening across the southern thrust front of the Greater Caucasus in western Georgia from kinematic modeling of folded river terraces above a listric thrust, *Earth and planetary science letters*, *544*, 116,362, doi: 10.1016/j.epsl.2020.116362.

Trexler, C. C., E. Cowgill, N. A. Niemi, D. A. Vasey, and T. Godoladze (2022), Tectonostratigraphy and major structures of the Georgian Greater Caucasus: Implications for structural architecture, along-strike continuity, and orogen evolution, *Geosphere*, *18*(1), 211–240, doi: 10.1130/GES02385.1.

Tye, A. R., N. A. Niemi, R. T. Safarov, F. A. Kadirov, and G. R. Babayev (2021), Sedimentary response to a collision orogeny recorded in detrital zircon provenance of Greater Caucasus foreland basin sediments, *Basin Research*, *33*(2), 933–967, doi: 10.1111/bre.12499.

Tye, A. R., N. A. Niemi, E. Cowgill, F. A. Kadirov, and G. R. Babayev (2022), Diverse deformation mechanisms and lithologic controls in an active orogenic wedge: Structural geology and thermochronometry of the eastern greater caucasus, *Tectonics*, *41*(12), e2022TC007,349, doi: 10.1029/2022tc007349.

van der Boon, A., D. J. J. van Hinsbergen, M. Rezaeian, D. Gürer, M. Honarmand, D. Pastor-Galán, W. Krijgsman, and C. G. Langereis (2018), Quantifying Arabia–Eurasia convergence accommodated in the Greater Caucasus by paleomagnetic reconstruction, *Earth and planetary science letters*, *482*, 454–469, doi: 10.1016/j.epsl.2017.11.025.

van Hinsbergen, D. J. J., T. H. Torsvik, S. M. Schmid, L. C. Maţenco, M. Maffione, R. L. M. Vissers, D. Gürer, and W. Spakman (2020), Orogenic architecture of the Mediterranean region and kinematic reconstruction of

its tectonic evolution since the Triassic, *Gondwana Research*, *81*, 79–229, doi: 10.1016/j.gr.2019.07.009.

Vasey, D. A., E. Cowgill, S. M. Roeske, N. A. Niemi, T. Godoladze, I. Skhirtladze, and S. Gogoladze (2020), Evolution of the greater caucasus basement and formation of the main caucasus thrust, georgia, *Tectonics*, *39*(3), e2019TC005,828, doi: 10.1029/2019tc005828.

Vasey, D. A., E. Cowgill, and K. M. Cooper (2021), A preliminary framework for magmatism in modern continental back-arc basins and its application to the Triassic-Jurassic tectonic evolution of the caucasus, *Geochemistry, Geophysics, Geosystems*, *22*(6), e2020GC009,490, doi: 10.1029/2020gc009490.

Vincent, S. J., A. C. Morton, A. Carter, S. Gibbs, and T. G. Barabadze (2007), Oligocene uplift of the Western Greater Caucasus: an effect of initial Arabia–Eurasia collision, *Terra nova*, *19*(2), 160–166, doi: 10.1111/j.1365-3121.2007.00731.x.

Vincent, S. J., A. Carter, V. A. Lavrishchev, S. P. Rice, T. G. Barabadze, and N. Hovius (2011), The exhumation of the western Greater Caucasus: a thermochronometric study, *Geological magazine*, *148*(1), 1–21, doi: 10.1017/S0016756810000257.

Vincent, S. J., W. Braham, V. A. Lavrishchev, J. R. Maynard, and M. Harland (2016), The formation and inversion of the western Greater Caucasus Basin and the uplift of the western Greater Caucasus: Implications for the wider Black Sea region, *Tectonics*, *35*(12), 2948–2962, doi: 10.1002/2016tc004204.

Vincent, S. J., M. L. Somin, A. Carter, G. Vezzoli, M. Fox, and B. Vautravers (2020), Testing models of cenozoic exhumation in the western greater caucasus, *Tectonics*, *39*(2), e2018TC005,451, doi: 10.1029/2018tc005451.

Yegorova, T., and V. Gobarenko (2010), Structure of the earth's crust and upper mantle of the west- and East-Black sea basins revealed from geophysical data and its tectonic implications, *Geological Society special publication*, *340*(1), 23–42, doi: 10.1144/sp340.3.

Zonenshain, L. P., and X. Le Pichon (1986), Deep basins of the Black Sea and Caspian Sea as remnants of Mesozoic back-arc basins, *Tectonophysics*, *123*(1-4), 181–211.

Zor, E. (2008), Tomographic evidence of slab detachment beneath eastern Turkey and the Caucasus, *Geophysical Journal International*, *175*(3), 1273–1282, doi: 10.1111/j.1365-246X.2008.03946.x.